Stability Analysis of an Active Mechanical Motion Rectifier for Wave Energy Conversion Systems

Pedro Fornaro[1,2]
[1]*Instituto LEICI*
Universidad Nacional de la Plata - CONICET
La Plata, Argentina
pedro.fornaro@mu.ie

John V. Ringwood[2]
[2]*Centre for Ocean Energy Research*
Department of Electronic Engineering - Maynooth University
Maynooth, Ireland
john.ringwood@mu.ie

***Abstract*—Recent literature proposes a novel Active Mechanical Motion Rectifier (AMMR) based power take-off system. The primary objective of mechanical rectification in wave energy conversion schemes is to ensure controlled unidirectional rotation speed in the generator, aiming to mitigate losses caused by low rotational speed and enhance overall system efficiency. Despite the promising potential of this proposal, ensuring the stability and controllability of the entire system remains an unresolved challenge. In that regard, this work addresses the former issue by providing a preliminary assessment of the stability of a flap operating with the proposed AMMR-based power take-off. The studies conducted in this work set the fundamental basis to facilitate the design of an effective controller for this novel power take-off system. The obtained results are validated through in-silico evaluations, modelling the system as piecewise linear.**

***Index Terms*—Wave energy conversion, flap, mechanical rectification, stability.**

I. Introduction

In recent years, extensive research has been conducted to meet the ever-growing energy demand and solve issues related to the availability and mixture of world energy sources. In particular, ocean waves contain renewable energy, which could serve as a critical resource towards a carbon-neutral society. The energy density of ocean waves is much higher than other renewable energy resources such as wind and solar [1]. Ideally, this high energy density can lead to ocean wave power plants with compact layouts, minimizing any environmental or social impacts.

Consequently, ocean wave energy has garnered substantial interest among researchers, giving rise to a multitude of innovative concepts and designs. However, the quest for the optimal wave energy conversion (WEC) device remains enshrouded in pervasive uncertainty, since both potential and kinetic energy forms can be harnessed [2]. In essence, WEC systems are composed of two distinctive parts: a wave capture body (WCB), and a power take-off (PTO). The former, transform the energy from the ocean into usable energy and can be classified into oscillating water columns, oscillating body devices, and overtopping devices. Irrespective of the employed WCB, the PTO subsystem assumes a crucial role in converting kinetic energy into electricity. The selection of an appropriate PTO type, along with an associated energy-maximising control algorithm, significantly influences the performance and efficiency of WECs.

Traditional PTOs can be categorized into direct-drive systems that employ linear or rotary electric generators, and indirect-drive systems that utilize hydraulic or mechanical transmission mechanisms. The utilization of a direct-drive linear generator presents an instinctive approach for converting mechanical energy into electricity, thereby garnering considerable interest among researchers. Hydraulic PTOs have found widespread adoption in multiple projects due to their inherent advantages, including robust power load capacity and well-established technological maturity. Lastly, rotary generators have demonstrated successful operation during extensive real-world testing.

Each of these traditional PTOs possesses distinct advantages. However, certain limitations have hindered their widespread implementation. For instance, hydraulic PTOs often encounter challenges related to sealing, leakage, scalability, and maintenance requirements. Linear electric generators, by comparison, exhibit larger physical mass due to the higher-rated force/torque on the machine. Rotary generators, on the other hand, tend to exhibit lower efficiency in the low-speed region, which is incongruent with the characteristics of ocean waves typically generating high force, but low velocity. In summary, the selection of an optimal PTO system, considering its strengths and weaknesses, plays an essential role in enhancing the overall performance and efficiency of WECs. Addressing the limitations of traditional PTOs is crucial for facilitating their wider adoption and realizing the full potential of ocean wave energy conversion.

In order to overcome the drawbacks of PTOs with mechanical transmissions, a mechanical motion rectifier (MMR) drivetrain has recently been developed [3]. In this design, one-way clutches are used to rectify a bidirectional motion, resulting in a unidirectional motion at the generator shaft. The MMR-based PTO has been tested with a point absorber [4] and a self-reacting two-body WCB [5]. In these preliminary results, significant improvement was reported in terms of wave-to-electricity efficiencies. Furthermore, the possibility to select the commutation intervals in an Active-MMR (AMMR) [6] [7], allows an active control law to synchronise the excitation force with the WCB velocity to be designed, maximising the power output.

While the AMMR shows promising results, it poses a challenge in designing a control algorithm that ensures optimal

power extraction. Additionally, stability analysis of the overall structure remains unexplored. In this work, we address the latter aspect by modelling the entire WEC as a switched system. Leveraging the systems inherent periodicity, and considering a linear feedback controller, we present preliminary results and tools to evaluate how the selection of the controller parameters and switching laws affect the stability of the overall system. This analysis lays the foundation for future work on this innovative AMMR-based PTO, providing a solid theoretical framework.

II. Description of the WEC system

This section presents a concise description of the employed WEC system. To that end, firstly, is presented and briefly discussed the AMMR operation principle. Secondly, the simplified dynamics of a flap operating as the selected WCB are presented. Finally, some considerations regarding the generator and control system are listed.

A. AMMR operation principle

The primary motivation of the AMMR is to keep the generator rotating unidirectionally (see Figure 1). To achieve this, the AMMR gearbox has two transmission modes to connect the flap and the generator. When a positive clutch is engaged, the generator and the flap move in the same direction. When a negative clutch is engaged, they move in the opposite direction, so that the generator always rotates unidirectionally despite the oscillating motion of the WCB.

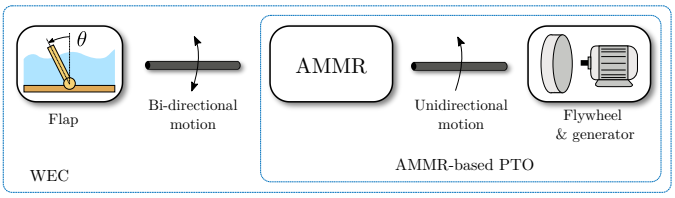

Figure 1. Illustrative WEC scheme including a flap WCB and a PTO conformed with the AMMR and a generator with interconnected flywheel.

Furthermore, it is possible to increase the efficiency of the generator by employing a flywheel to increase its inertia and maintain a higher average velocity. As shown in [4], the AMMR mechanism can increase power outputs with simple linear damping control. This power increase is attributed to a unique disengagement phenomenon where the generator is decoupled from the WCB during parts of the excitation period. However, disengaging the generator from the rest of the system implies that the WCB remains effectively uncontrolled for part of the wave cycle.

Naturally, controlling the phases of disengagement/ engagement is the key to both controlling the system and guaranteeing its stability. To address this challenge, the designed AMMR [6] uses controllable electromagnetic clutches in place of the one-way clutches in the MMR, making disengagement fully controllable [8]. Employing this structure, in [7] it was proven that, considering different excitation frequencies, the switching law can be designed to optimise power extraction by synchronising the WEC velocity with the excitation force. This system increases the design freedom and extends the control design scope to include not only the generator force but also the commutation periods.

In this work, the AMMR is considered ideal. This implies that the system is capable of instantly, and free of losses, connecting or disconnecting the generator from the WCB.

B. Simplified WCB dynamics

In this work, a simple flap is assumed (Figure 1). When the AMMR clutches are engaged, the system is connected to the generator through a mechanical drivetrain. Then, assuming narrow-banded excitation, an approximate linear model for the motion of such a device for $t \in \mathbb{R}^+$ is [7]:

$$J_T(\omega)\ddot{\theta} = -B(\omega)\dot{\theta} - K\theta + f_{ex} + u \tag{1a}$$

$$y = \dot{\theta}, \tag{1b}$$

where θ is the device excursion (displacement), $\dot{\theta}$ and $\ddot{\theta}$ are the device angular velocity and acceleration respectively. Also, u is the control action, which is a force supplied by means of the PTO system. On their part, the frequency-dependant therms are $J_T(\omega)$, which represents the total inertia of the system considering the generator inertia as well, and $B(\omega)$ which is the so-called radiation damping [9]. f_{ex} denotes the wave excitation force, i.e., an external uncontrollable input due to the incoming wave. Finally, the hydrostatic stiffness coefficient K (articulating the balance between the gravity and static buoyancy forces on the WCB) is assumed to be constant, which is a good approximation when the displacement θ is small [10]. When both clutches are open, and the generator is disengaged, the WCB dynamics take the following form [7]:

$$J_P(\omega)\ddot{\theta} = -B(\omega)\dot{\theta} - K\theta + f_{ex} \tag{2a}$$

$$y = \dot{\theta}, \tag{2b}$$

where $J_P(\omega)$ is the total inertia of the disengaged system, i.e., without considering the generator and flywheel inertia. It is worth noting that the AMMR-controlled system has two distinctive operation modes. The first one is when the clutches are disengaged, in which essentially the system remains in an open-loop configuration and $u = 0$. The second operation mode appears with the electromagnetic clutches engaged, and in that case, $u \neq 0$, and both the generator and flywheel inertia need to be considered. These aspects are further developed in Section III, where it is shown that is possible to obtain a unified description for the WEC by employing concepts of switched systems.

C. Generator and controller considerations

The generator electromagnetic torque can be controlled in a wide variety of ways. The harvested electrical power is the mechanical power input to the generator rotor minus generator and power electronics losses. In this work, these losses are neglected and only mechanical power is considered. In this way, the analysis is focused on the stability of the mechanical

part of the WEC, considering the hydrodynamic modelling of WCB interaction and connected PTO dynamics.

During the engagement stages, the generator has a crucial role in guaranteeing the system stability, and also to harvest energy from the incoming waves. In that regard, the selected control action is essential, since the general objective of control, in the wave energy context, is to maximise converted energy. To establish a simple WEC control capable to act on the WCB during the engagement stages, the WCB motion is described in terms of Equation (1). With this assumption, a classical control structure based on the so-called impedance matching principle (which is a well-known strategy within the electrical and electronic engineering community), is designed to obtain maximum power transfer [11]. Employing this concept, a simple feedback controller to maximise energy extraction is a proportional + integral (PI) controller, whose parameters can be adjusted in a wide variety of ways [9]. The structure of this control system can be appreciated in Figure 2. In essence, the controller affects the stiffness and damping coefficients of the system depending on the selected values for the proportional k_p, or integral k_i gains, to match the natural oscillating frequency of the system with the frequency of the excitation force. Then, assuming narrow-banded excitation, the PI controller parameters can be selected as:

$$k_i = k_1 \omega^2 (J_T(\omega)) - K \tag{3a}$$

$$k_p = k_2 B(\omega), \tag{3b}$$

where the parameters k_1 and k_2 are auxiliary gains. In this work, the goal is to evaluate how the controller parameters might affect the stability of the complete system. This is addressed in Section IV, varying the parameters k_1 and k_2.

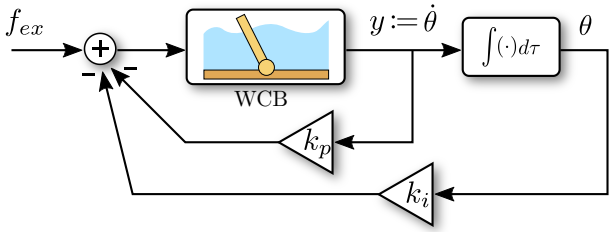

Figure 2. Block diagram of the PI controller scheme during the engagement stage.

III. Switched system description and stability analysis of the AMMR-based WEC

In this section, the stability of the AMMR-based WEC is presented. To that end, initially, a unified description of the WEC dynamics is defined. Then, the tools employed to analyse the system stability are presented.

A. Unified WEC model including the AMMR-based PTO

In this subsection, a complete unified model for the AMMR-based PTO and WCB is developed. To simplify this preliminary analysis, the generator dynamics are neglected. Assuming that θ is the angular displacement of the flap, then the unified dynamics of the system are given by:

$$J_{\sigma(\theta,t)}\ddot{\theta} = -B(\omega)\dot{\theta} - K\theta + f_{ex} + u_{\sigma(\theta,t)} \tag{4a}$$

$$y = \dot{\theta}, \tag{4b}$$

In this system description, the set $\sigma(\theta, t) : \mathbb{R}^n \times \mathbb{R}^+ \to \{0, 1\}$ is the so-called switching function. It is used to indicate how the switching law affects the dynamics, depending on the electromagnetic clutches states. For instance, when the clutches are disengaged, $\sigma(\theta, t) = 0$ and J_0 is equal to the inertia of the WCB and $u_0 = 0$, i.e., there is no control action applied to the system. However, when the clutches are engaged, $\sigma(\theta, t) = 1$ and J_1 equals the total inertia of the system considering the flywheel and generator inertia, and $u_1 = f(\theta, \dot{\theta})$, i.e., a control action as a function of the system states can be employed to control the WCB velocity and position, by means of the generator torque.

Although, in conventional WEC systems, the only control action is the PTO force, in this configuration, it is also possible to use the switching function as a stabilizing and control parameter to be designed. The effects of considering different switching laws have been analysed and discussed in [7]. However, in [7], the control action is assumed to operate as a simple passive controller with $u_1 = -k_p\dot{\theta}$, and no considerations regarding system stability were made. With that in mind, in the following section, the system stability is thoroughly analysed. Before proceeding with this analysis, the switched system is described using the state-space representation:

$$\dot{\mathbf{x}} = \mathbf{A}_{\sigma(x,t)}\mathbf{x} + \mathbf{B}_{\sigma(x,t)}u_{\sigma(x,t)} = \tag{5a}$$

$$\begin{bmatrix}\dot{x}_1\\ \dot{x}_2\end{bmatrix} = \begin{bmatrix}0 & 1\\ \frac{-K}{J_{\sigma(x,t)}} & \frac{-B}{J_{\sigma(x,t)}}\end{bmatrix}\begin{bmatrix}x_1\\ x_2\end{bmatrix} + \begin{bmatrix}0\\ \frac{1}{J_{\sigma(x,t)}}\end{bmatrix} u_{\sigma(x,t)}$$

$$y = \mathbf{C}_{\sigma(x,t)}\mathbf{x} + \mathbf{D}_{\sigma(x,t)}u_{\sigma(x,t)} = \begin{bmatrix}0 & 1\end{bmatrix}\begin{bmatrix}x_1\\ x_2\end{bmatrix}, \tag{5b}$$

where $[x_1\, x_2]^\intercal := [\theta\, \dot{\theta}]^\intercal$.

B. Stability analysis

In this section, the stability of the switched AMMR-based PTO is analysed. Conventionally, the switched system stability is highly dependent on the employed switching law. However, in the case under study, the system is periodic, and the switching law takes a finite number of values (in this case 0 or 1) four times per period of the $f_{ex}(t)$ and during fixed intervals δt_i (see Figure 3). Consequently, as discussed in this section, the system stability can be analysed in terms of the transition matrix of a single period of the excitation force.

Before proceeding with the method employed to determine the system stability, it is necessary to remark that this proposal is aligned with classical Lyapunov stability concepts, as discussed in [12]. Assume that $x(t)$ is the solution of the system for a given initial condition $x(0)$. Then the origin is stable, in the Lyapunov sense, if:

- There exist $\epsilon > 0$ and $r > 0$ such that for any $|x(0)| \leqslant r$ then $|x(t)| \leqslant \epsilon$ for each solution, and $\forall\, t > 0$.

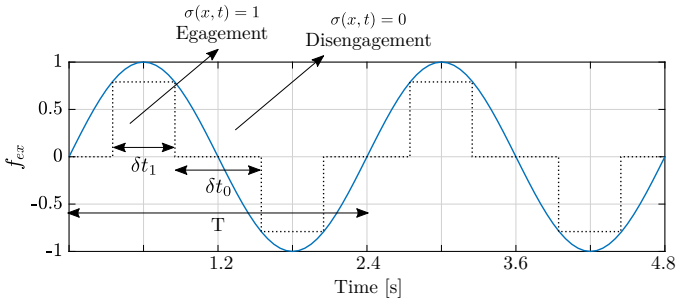

Figure 3. Sinusoidal excitation force with period $T = 2.4s$, and illustrative example of a possible commutation law.

- Furthermore, the origin is also locally attractive if all solutions $x(t)$ with $x(0)$ sufficiently close to the origin are such that $x(t) \to 0$ as $t \to \infty$.

For further discussion, and a more general stability definition for switched systems, please refer to [12]. Consequently, the stability of the system is limited to the analysis of the evolution of the system states in one single period of the excitation force [13]. In essence, the proposal requires evaluating if, in a single cycle, the trajectories described by the states of the model approach zero, i.e., if the system trajectories are contractive. Since the system can be analysed as piecewise linear, the null response in a period is [14]:

$$x(T + t_0) = \prod_{i=N}^{1} e^{A_i \delta t_i} x(t_0), \tag{6}$$

with $N = 4$ being the number of switchings actions in one period, and $e^{A_i \delta t_i}$ the transition matrix of the $i\text{-}th$ interval of length δt_i, computed with its correspondent matrix from Equation (5). If the null solution tends to zero, then the absolute value of the eigenvalues of the transition matrix evaluated in $t = T + t_0$ must be smaller than one:

$$|\lambda_{MAX}\left(\Phi(T + t_0, t_0)\right)| = |\lambda_{MAX}\left(\prod_{i=4}^{1} e^{A_i \delta t_i}\right)| < 1, \tag{7}$$

It is fundamental to remark that the stability of two interconnected linear constant and stable systems, might be affected by the employed switching law. Specifically, the interconnection of two stable linear systems might result in an unstable system [12] [13]. Also, in the case under study, the dynamics of the system are affected by the feedback controller with the clutches engaged, and the WCB has free movement with the clutches disengaged. Therefore, the stability of the full system depends on both the employed control law and the switching law.

IV. Results and Discussion

In this section, the results of the stability analysis for the proposed AMMR-based PTO are presented. To simplify the presentation of the results, two different cases are separately analysed. In each case, the absolute value of the maximum eigenvalue of the transition matrix is computed (Equation (7)). Firstly, considering a constant proportional gain k_p, and both a variable switching law and variable integral gain k_i which is modified considering $k_1 = 1, 2, ..., 10$. Secondly, this analysis is repeatedly conducted considering different values for the proportional gain, obtained considering $k_2 = 1, 2, 3$.

Table I
Flap WCB and PI parameters for different fundamental wave periods.

Wave period [s]	**Inertia** [kgm^2]	**Damping** [Nms/rad]	**Stiffness** [Nm/rad]	$\mathbf{k_{p0}}$	$\mathbf{k_{i0}}$
2.4	77	75	285	75	256
3	68	57	285	57	22
4.3	50	61	285	61	-174

Furthermore, since in this preliminary study, the excitation force is regarded as pure sinusoidal, the stability analysis is also conducted considering different periods for the excitation force. This latter aspect is required, since changes in the frequency of f_{ex} result in changes in the frequency-dependant system coefficients, such as added mass and damping. In Table I, a list of values for a flap with different fundamental periods of the excitation force is presented. Consequently, the PI controller coefficients are also adjusted with the frequency of f_{ex}, consistent with Equation (3).

In a wave period (T), the intervals T_{off} and T_{on} correspond to the disengagement and engagement stages respectively. It is also worth noting that there are two boundary conditions in which the system is inherently stable, i.e., when $T_{off} = 0$, $T_{on} = T/2$ and $T_{off} = T/2$, $T_{on} = 0$, when the system is not switching.

A. Case 1: Effects of varying the integral gain of the controller

In this first case, the effects of varying the integral gain k_i of the PI controller are evaluated while the proportional gain remains constant. In this situation, the maximum eigenvalue of the transition matrix, over one period, is numerically computed by sweeping the complete interval $T_{off} \in [0; T/2]$ (since, over half a period, there are two switches, as presented in Figure 3). The results of this evaluation can be appreciated in Figure 4. Note that this process is repeated considering the three wave periods from Table I.

It is worth noting that, in the case $k_1 = k_2 = 1$, the parameters of the PI guarantee maximum power extraction if $T_{off} = 0$. Aligned with this aspect, it is remarked that employing negative gains in the controller results in the rapid instability of the whole system due to the existence of eigenvalues of the controlled system with positive real parts, and therefore only the cases in which the gains (k_1 and k_2) are positive are analysed.

It can be appreciated that varying the controller coefficient k_i (by means of k_1) has a major impact on the system stability. The switching conditions for which the system remains stable, are considerably reduced with a larger k_1. However, considering different wave periods also affects the system stability; waves with a larger period exhibit greater stability for the same value of k_i.

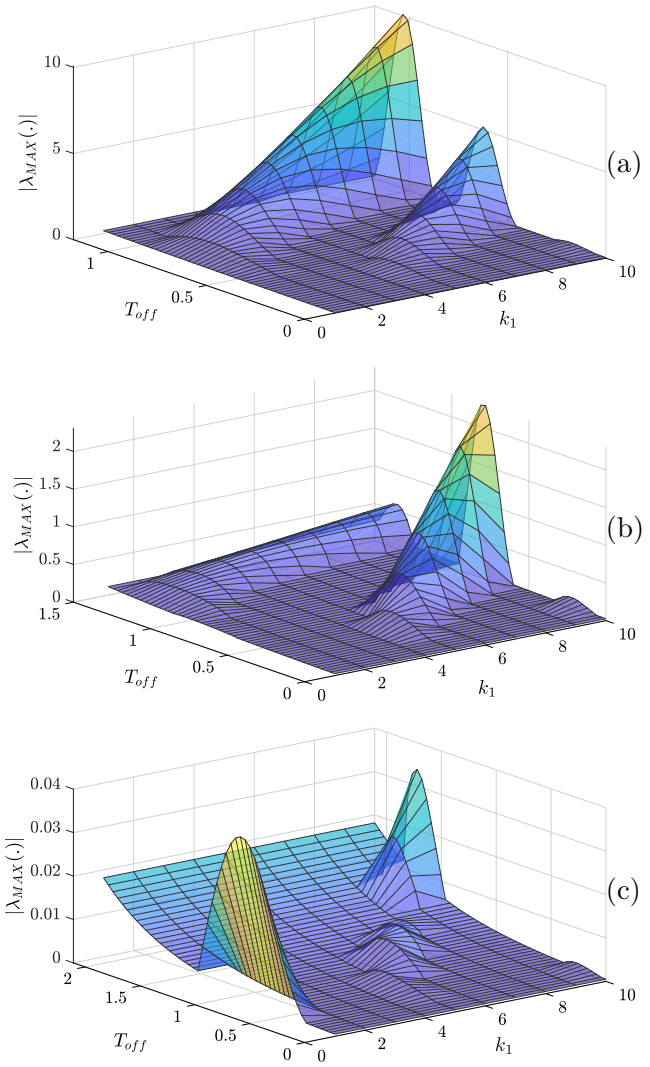

Figure 4. Absolute value of the maximum eigenvalue of the transition matrix $\Phi(T + t_0, t_0)$ for different wave excitation periods, plotted as a function of the switching law and controller proportional gain. a) $T = 2.4s$. b) $T = 3s$. c) $T = 4.3s$.

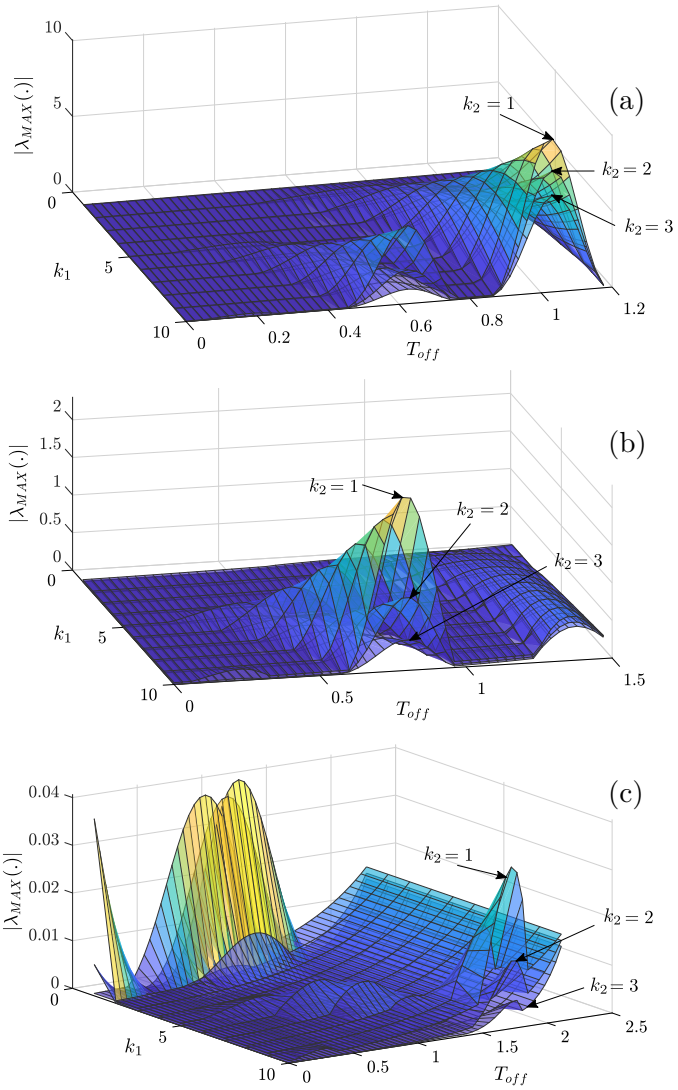

Figure 5. Absolute value of the maximum eigenvalue of the transition matrix $\Phi(T + t_0, t_0)$ for different wave excitation periods, plotted as a function of the switching law, and the controller proportional and integral gains. a) $T = 2.4s$. b) $T = 3s$. c) $T = 4.3s$.

B. Case 2: Effects of varying the proportional gain of the controller

In this second case, the effects of varying the proportional gain k_p of the PI are evaluated. Analogously to the previous case, the maximum eigenvalue of the transition matrix, over one period, is numerically computed considering $T_{off} \in [0; T/2]$. The results of this evaluation can be appreciated in Figure 5. As in the previous case, this process is evaluated considering the three wave periods from Table I.

In this analysis, the system stability is also seen to be very sensitive to variations in the proportional gain. However, in this case, increasing the gain k_2 results in systems that are more stable for the same gain k_1. From the point of view of classical wave energy control, this is directly connected with the fact that the proportional gain controls the system damping. Therefore, increasing this parameter also increases the dissipative effects of the system, simultaneously increasing the overall system stability.

C. Illustrative numerical example

To complement the previous analysis, an illustrative example is now presented. Assume that $T = 3s$, $k_1 = 10$, and $k_2 = 1.5$. Then, evaluating the absolute value of the maximum eigenvalue from Equation (6), for different values of T_{off} results in Figure 6, where it can be seen that if $T_{off}2/T$ is approximately in the interval $[0.48; 0.59]$, then the system is unstable.

To verify this assumption, the system is simulated considering initial conditions $[x_1; x_2]^\intercal = [2; 3]^\intercal$. Then, the phase plane of position vs velocity can be appreciated in Figure 7. Figure 7.a illustrates how, with $T_{off} = 0.58$, the system is unstable with $|\lambda_{MAX}(\Phi(T, 0))| = 1.04$ and, as

$t \to \infty$, the trajectories are dragged away from the origin. On the other hand, Figure 7.b shows how increasing T_{off} to 0.6, encourages the trajectories to approach the origin since $|\lambda_{MAX}\left(\Phi(T,0)\right)| \approx 0.6$.

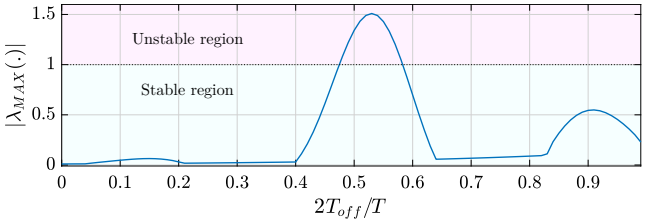

Figure 6. Absolute value of the maximum eigenvalue of the transition matrix $\Phi(T+t_0,t_0)$ for the illustrative example with $T=3s$, $k_1=10$ and $k_2=1.5$.

It is worth noting that evaluating the stability of the system for different controller parameters is essential, even though for the AMMR-based PTO, there is still no consensus regarding the optimal control strategy.

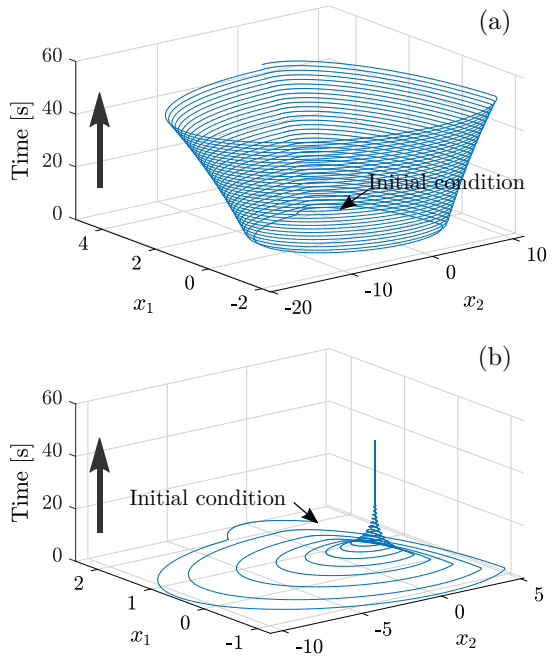

Figure 7. Phase plane of the WCB states parametrised as a function of time. a) Unstable system with $T_{off}=0.58$. b) Stable system with $T_{off}=0.6$

V. Conclusions

In this work, a preliminary analysis of the stability of a novel AMMR-based PTO was presented. Employing elements from linear time-varying systems and taking advantage of the inherent periodicity of the system, in this work it was possible to establish tools to evaluate the stability of the system. The preliminary theoretical results were validated by simulation considering a flap WCB. To model this system, a monochromatic excitation was assumed to employ the spring, mass and damper second-order frequency-dependant model.

Then, to assess the system stability over a wide operating range, an empirical evaluation of the eigenvalues of the transition matrix over one period of the excitation force was conducted. In this analysis, during the engagement periods, the PTO employs a simple PI to control the WCB, and a broad range of parameters to tune the controller was also considered.

The new mechanical rectifier possesses great potential to increase the power output of PTOs but presents challenges from the control theory viewpoint. Specifically, the structure of the system is inherently a switching one increasing the difficulty of the analysis of controllability, observability and stability. In that regard, the preliminary analysis developed in this work lays a foundational theoretical background for future work in the area.

Acknowledgements

This work was possible thanks to the support of the University Nacional de La Plata, La Plata, Argentina, and Science Foundation Ireland under grant number 21/US/3776.

References

[1] J. V. Ringwood, G. Bacelli, and F. Fusco, "Energy-maximizing control of wave-energy converters: The development of control system technology to optimize their operation," *IEEE Control Systems*, vol. 34, no. 5, pp. 30–55, 2014.

[2] B. Guo and J. V. Ringwood, "A review of wave energy technology from a research and commercial perspective," *IET Renewable Power Generation*, vol. 15, no. 14, pp. 3065–3090, 2021.

[3] C. Liang, J. Ai, and L. Zuo, "Design, fabrication, simulation and testing of an ocean wave energy converter with mechanical motion rectifier," *Ocean Engineering*, vol. 136, pp. 190–200, may 2017.

[4] X. Li, C. Chen, Q. Li, L. Xu, C. Liang, K. Ngo, R. G. Parker, and L. Zuo, "A compact mechanical PTO for wave energy converters: Design, analysis, and test verification," *Applied Energy*, vol. 278, p. 115459, nov 2020.

[5] X. Li, D. Martin, C. Liang, C. Chen, R. G. Parker, and L. Zuo, "Characterization and verification of a two-body wave energy converter with a novel PTO," *Renewable Energy*, vol. 163, pp. 910–920, jan 2021.

[6] L. Yang, J. Huang, N. Congpuong, S. Chen, J. Mi, G. Bacelli, and L. Zuo, "Control co-design and characterization of a power takeoff for wave energy conversion based on active mechanical motion rectification," *IFAC-PapersOnLine*, vol. 54, no. 20, pp. 198–203, 2021.

[7] L. Yang, J. Huang, J. Mi, M. Hajj, G. Bacelli, and L. Zuo, "Optimal power analysis of a wave energy converter with a controllable power takeoff based on active motion rectification," *IFAC-PapersOnLine*, vol. 55, no. 27, pp. 299–304, 2022.

[8] P. Fornaro and J. V. Ringwood, "On the controllability of an active mechanical motion rectifier for wave energy converters," in *2024 American Control Conference*, 2024.

[9] F. Fusco and J. V. Ringwood, "A simple and effective real-time controller for wave energy converters," *IEEE Transactions on Sustainable Energy*, vol. 4, no. 1, pp. 21–30, jan 2013.

[10] D. Crooks, "Nonlinear hydrodynamic modelling of an oscillating wave surge converter," Ph.D. dissertation, Queen's University Belfast, 2017.

[11] J. V. Ringwood, S. Zhan, and N. Faedo, "Empowering wave energy with control technology: Possibilities and pitfalls," *Annual Reviews in Control*, vol. 55, pp. 18–44, 2023.

[12] R. Goebel, *Hybrid dynamical systems modeling, stability, and robustness*. Princeton University Press, 2012.

[13] J. Ezzine and A. H. Haddad, "Controllability and observability of hybrid systems," *International Journal of Control*, vol. 49, no. 6, pp. 2045–2055, jun 1989.

[14] M. S. Hossain and S. Trenn, "A time-varying gramian based model reduction approach for linear switched systems," *IFAC-PapersOnLine*, vol. 53, no. 2, pp. 5629–5634, 2020.